

Andreev spectroscopy of Majorana states in topological superconductors with multipocket Fermi surfaces

Ana C. Silva¹, Miguel A. N. Araújo^{1,2,3} and Pedro D. Sacramento^{1,3}

¹ *CFIF and CeFEMA, Instituto Superior Técnico,*

Universidade de Lisboa, Av. Rovisco Pais, 1049-001 Lisboa, Portugal

² *Departamento de Física, Universidade de Évora, P-7000-671, Évora, Portugal and*

³ *Beijing Computational Science Research Center, Beijing 100089, China*

The topological properties of a multiband topological superconductor in two dimensions are studied, when the latter is obtained by introducing electron pairing in an otherwise topological insulator. The type of pairing, doping and Fermi surface topology play an essential role. Considering the Andreev reflection problem, we use a previously developed quantum waveguide theory for multiorbital systems and find that, when the Fermi surface has several pockets, this theory retrieves the correct number of Majorana fermion states as predicted by the topological index. By varying band structure parameters, the Fermi surface topology of the normal phase can be made to change, whereby the number of Majorana modes also varies. We calculate the effect of such transitions on the Andreev differential conductance.

PACS numbers: 71.10.Fd, 71.10.Pm, 71.10.Li, 73.20.-r, 74.45.+c, 74.20.Rp

I. INTRODUCTION

Recent interest in non-trivial topological properties of insulators¹ has spurred intensive research on band models displaying non-trivial topology². In the case of superconductivity, non-trivial topology is associated with the emergence of zero energy excitations which are their own antiparticles, or Majorana fermions (MFs). Condensed matter therefore provides the ground for the realization of such long sought exotic particles^{3,4}.

Early theoretical models of two-dimensional topological superconductivity consider $p + ip$ pairing in an otherwise trivial band. In such a framework, the emergence of MFs in spinless fermion models was shown to be related to topology⁴. Non-abelian MF's were shown to arise at vortex cores in a model of spinfull fermions with spin triplet $p + ip$ pairing and where the two spin components effectively decouple⁵. It is this concept of MF that we shall deal with, in this work. Besides their interest from the point of view of fundamental physics, the MF's non-Abelian exchange statistics is their most remarkable property and suitable for quantum computation applications⁶. It was early realized that an effective $p + ip$ superconductor arises from single band Dirac electrons complemented with s-wave pairing⁷. A promising venue for the construction of topological superconductors is the proximity coupling of a topological insulator to a superconductor^{8,9}. The possibility of engineering topological superconductors using the surface of a three-dimensional TI or a two-dimensional semiconductor in proximity to a s-wave superconductor was discussed⁸ but multiorbital effects were not considered. Non-conventional superconductivity and Andreev reflection were also studied¹⁰. We note that topological materials are necessarily multiorbital. The consideration of $p + ip$ (or other) pairing in a single band model is therefore a simplification.

More recently, there has been interest in multior-

bit systems. The orbital degree of freedom (pseudospin) is present in a lattice symmetry transformation, namely, that of lattice inversion, and the characterization of pairing term as having even/odd parity under inversion. Such investigations have been motivated by the three-dimensional topological superconductor $\text{Cu}_x\text{Bi}_2\text{Se}_3$, which has two orbitals per lattice cell. Some theorems on the topological indices to be expected for various superconductor models, by taking their symmetries into account, have recently been established. In many cases, the topology of the Fermi surface itself is important. For instance, under the assumption of lattice inversion symmetry, time-reversal invariance (TRI) and odd parity pairing, three-dimensional superconductors are topological if they possess an odd number of Fermi surface pockets^{11,12}. Models of two-dimensional superconductors with a pseudospin degree of freedom have been proposed recently, concentrating on the case of nodeless odd parity pairing in TRI superconductors. In this case non-trivial topology requires spin-orbit couplings non-diagonal in the pseudospin channel^{13,14}.

we introduce below a model for a superconductor which has two orbitals per lattice site. For the case of diagonal (in pseudospin space) pairing, we find that the topological properties of the kinetic energy have no influence on those of the superconductor. The latter are determined, instead, by the pairing symmetry and the Fermi surface (FS) topology. We also study the Andreev problem at the normal/superconductor (N/S) boundary, assuming the normal metal to be single band, using the previously established quantum waveguide theory (QWT). QWT was originally developed to address the Andreev reflection problem in heavy-fermion superconductors^{15,16} and, later on, iron pnictide superconductors¹⁷⁻²⁰. It can be applied when the N/S interface is parallel to one the primitive vectors of the superconductor and normal metal. For other interface angles, other approaches have to be employed. QWT also ignores the detailed micro-

scopic behavior of hopping parameters at the interface. Refinements of this theory which consider fully microscopic behavior of hopping parameters can be found in Refs^{21,22}.

While the Blonder-Tinkham-Kapljwick (BTK) theory²³ predicts a zero energy Andreev bound state (ABS) for each FS pocket, QWT accounts for the quantum interference effects between different FS pockets. As we shall see below, the ABS predicted by QWT correctly reconciles the Andreev problem with the topological index.

II. MULTIORBITAL SUPERCONDUCTOR

A. Pairing in a two-dimensional TI

The simplest version of superconducting pairing is that where electrons with opposite spins are related by time-reversal in the normal phase. The model includes at least two orbitals per lattice site (pseudo-spin) in addition to the spin degree of freedom. In the simplest version, the spin \uparrow electrons have kinetic energy $\Xi_{\uparrow}(\mathbf{k})$ which is related to that of the spin \downarrow electrons by time-reversal, $\Xi_{\downarrow}(\mathbf{k}) = \Xi_{\uparrow}^*(-\mathbf{k})$. If Ξ_{\uparrow} has an odd Chern number then the normal system serves as a model for a TI in two dimensions¹. In the case of two orbitals per lattice cell, we can write

$$\Xi_{\uparrow}(\mathbf{k}) = \mathbf{h}(\mathbf{k}) \cdot \boldsymbol{\tau} + h_0(\mathbf{k})\tau_0 \quad (1)$$

where the Pauli matrices $\tau_{i=1,2,3}$ act on orbital space (pseudo-spin) and τ_0 denotes the identity matrix. We shall later use Pauli matrices σ_i , t_i and r_i operating on spin, particle-hole and Bogolubov-de Gennes amplitude $(u \ v)$ spaces, respectively.

The Bogolubov-de Gennes (BdG) matrix in the particle-hole basis $(\hat{c}_{\uparrow}\hat{c}_{\downarrow}\hat{c}_{\uparrow}^{\dagger}\hat{c}_{\downarrow}^{\dagger})$, where the field operators \hat{c}_{σ} include the pseudo-spin degrees of freedom, takes the form:

$$\mathcal{H} = \begin{pmatrix} \hat{\Xi} & \hat{\Delta} \\ \hat{\Delta}^{\dagger} & -\hat{\Xi}^T \end{pmatrix}, \quad (2)$$

where $\hat{\Xi} = \text{diag}(\Xi_{\uparrow}, \Xi_{\downarrow})$. Keeping spin s_z as a good quantum number, the pairing matrix $\hat{\Delta}$ can have singlet $\psi(\mathbf{k})i\sigma_2$ and triplet $d_z(\mathbf{k})\sigma_1$ components. The form of the the pairing matrix in pseudospin space remains to be chosen. We shall write

$$\hat{\Delta}(\mathbf{k}) = (\Delta_s \psi(\mathbf{k})i\sigma_2 + \Delta_t d_z(\mathbf{k})\sigma_1) \tau_j, \quad (3)$$

where the Pauli matrix τ_j remains to be specified. Then \mathcal{H} splits into two BdG matrices for $(\hat{c}_{\uparrow}\hat{c}_{\downarrow}^{\dagger})$ and $(\hat{c}_{\downarrow}\hat{c}_{\uparrow}^{\dagger})$ spaces. The former reads

$$H = (\mathbf{h}(\mathbf{k}) \cdot \boldsymbol{\tau} + h_0(\mathbf{k})\tau_0) r_3 + \text{Re}[\Delta(\mathbf{k})] \tau_j r_1 - \text{Im}[\Delta(\mathbf{k})] \tau_j r_2, \quad (4)$$

We next study the topological indices of (4). We first consider diagonal pairing in orbital space, $\tau_j = \tau_0$. In

this case the eigenfunctions of (4) can be written as a direct product

$$\begin{pmatrix} (u_{\uparrow}) \\ (v_{\downarrow}) \end{pmatrix} = \begin{pmatrix} u \\ v \end{pmatrix} \otimes \begin{pmatrix} \alpha \\ \beta \end{pmatrix} \quad (5)$$

Wave function normalization reads $|u|^2 + |v|^2 = |\alpha|^2 + |\beta|^2 = 1$. The amplitudes (α, β) diagonalize the kinetic energy

$$[\mathbf{h}(\mathbf{k}) \cdot \boldsymbol{\tau} + h_0(\mathbf{k})\tau_0] \begin{pmatrix} \alpha \\ \beta \end{pmatrix} = \xi(\mathbf{k}) \begin{pmatrix} \alpha \\ \beta \end{pmatrix}, \quad (6)$$

and the BdG amplitudes (u, v) obey

$$\mathbf{h}' \cdot \mathbf{r} \begin{pmatrix} u \\ v \end{pmatrix} = E(\mathbf{k}) \begin{pmatrix} u \\ v \end{pmatrix}. \quad (7)$$

Where we have defined the vector \mathbf{h}' components as $h'_x - ih'_y = \Delta(\mathbf{k})$ and $h'_z = \xi(\mathbf{k})$. The two normal state bands are $\xi(\mathbf{k}) = \pm|\mathbf{h}(\mathbf{k})| + h_0(\mathbf{k})\tau_0$. The Berry connection obtained from (5) is

$$\begin{aligned} \mathcal{A} &= i((u_{\uparrow})^{\dagger} (v_{\downarrow})^{\dagger}) \frac{\partial}{\partial \mathbf{k}} \begin{pmatrix} (u_{\uparrow}) \\ (v_{\downarrow}) \end{pmatrix} \\ &= i(u^* \ v^*) \frac{\partial}{\partial \mathbf{k}} \begin{pmatrix} u \\ v \end{pmatrix} + i(\alpha^* \ \beta^*) \frac{\partial}{\partial \mathbf{k}} \begin{pmatrix} \alpha \\ \beta \end{pmatrix} \\ &\equiv \mathbf{a}' + \mathbf{a} \end{aligned} \quad (8)$$

where \mathbf{a}' and \mathbf{a} denote Berry connections associated with $(u \ v)$ and $(\alpha \ \beta)$, respectively. The total Chern number, C , is given by the line integral around the BZ,

$$C = \sum \oint \mathcal{A} \cdot \delta \mathbf{k} \quad (9)$$

$$= \sum \oint \mathbf{a}' \cdot \delta \mathbf{k} + \sum_{\pm} \oint \mathbf{a} \cdot \delta \mathbf{k} \quad (10)$$

where the summation in (9) is over the two negative BdG bands $E_{\pm}(\mathbf{k}) = -\sqrt{\xi_{\pm}^2(\mathbf{k}) + |\Delta(\mathbf{k})|^2}$ of the eigenproblem (7). The summation in the second term of equation (10) is the Chern number of the two normal bands $\xi(\mathbf{k})$ and therefore equates to zero. Hence we find that *the topology of Ξ_{\uparrow} does not contribute to C* because of cancelation in the sum over the normal state bands. It remains to analyse the first term in equation (10). Using Stokes theorem, the line integral of \mathbf{a}' can be written as the flux of a monopole $\Omega' = \nabla \times \mathbf{a}' = \hat{\mathbf{h}}'/(2h'^2)$, through the Bloch sphere:

$$C = \frac{1}{2\pi} \sum \int \Omega' \cdot d\mathbf{S}'_{\mathbf{k}}. \quad (11)$$

Here, $\mathbf{h}' = (\text{Re}\Delta(\mathbf{k}), \text{Im}\Delta(\mathbf{k}), \xi_{\pm})$ are the two monopoles' curvature fields. The vector \mathbf{h}' covers the Bloch sphere C times. The north (N) and south (S) hemispheres correspond to $h'_z = \xi$ being either positive or negative. If the chemical potential, which is included in h_0 ,

lies in the gap between the normal ξ_{\pm} bands, then $C = 0$ because \mathbf{h}' stays always in one hemisphere. *Nonzero C requires the chemical potential to intercept at least one of the normal bands (ξ_{-} or ξ_{+}) and the N/S hemispheres are attained when h'_z is outside or inside FS pockets. This links C to the topology of the FS.* The other normal band does not contribute to C . The N and S poles are attained at BZ points where $h'_x \pm ih'_y = \Delta^{(*)}(\mathbf{k})$ vanishes. This motivates the choice of $p + ip$ pairing below. A relevant example of a multiband superconductor believed to have $p + ip$ symmetry is Sr_2RuO_4 ^{24,25}

We recall that a theorem relating the topological indices of a superconductor to the FS topology has been established by Sato²⁶ for the case where the normal bands have inversion symmetry and pairing has odd parity. Our discussion above makes no requirement on inversion symmetry or parity. In the case of time-reversal invariant single band spin triplet superconductors, the topological indices were also shown to be related to FS topology²⁷.

For other choices of τ_j in equations (3)-(4) the direct product form (5) is no longer valid. We shall address those cases below by computing winding numbers for TRI momenta where H is chiral.

B. Model

We write kinetic energy for \uparrow -spin electrons as in equation (1), where

$$\begin{aligned} h_x &= \sin k_y, & h_y &= -\sin k_x, \\ h_z &= 2t_1(\cos k_x + \cos k_y) + 4t_2 \cos k_x \cos k_y, \\ h_0 &= -\mu - t_1(\cos k_x + \cos k_y). \end{aligned} \quad (12)$$

We consider a spin triplet $p + ip$ pairing:

$$\hat{\Delta}(\mathbf{k}) = d_z(\mathbf{k})\sigma_1 \otimes \tau_0, \quad (13)$$

with $d_z(\mathbf{k}) = \Delta(\sin k_x - i \sin k_y)$. The pairing term (13) has odd parity under inversion. This symmetry property reads¹¹: $\tau_1 \hat{\Delta}(-\mathbf{k}) \tau_1 = -\hat{\Delta}(\mathbf{k})$.

In the absence of Rashba or Dresselhaus spin-orbit couplings the Bogolubov-deGennes matrix in the particle-hole basis, $\left((\hat{c}_{\uparrow})(\hat{c}_{\downarrow})(\hat{c}_{\uparrow}^{\dagger})(\hat{c}_{\downarrow}^{\dagger}) \right)$, splits into two 4×4 matrices. We consider now only the subspace $\left((\hat{c}_{\uparrow})(\hat{c}_{\downarrow}^{\dagger}) \right)$. The parameter choice $\mu = 0.6$, $t_1 = 0.07$, $t_2 = -0.08$, produces a FS with 3 pockets centered at $(0, 0)$, $(0, \pi)$, $(\pi, 0)$ in the Brillouin Zone (BZ), as figure 1 (left panel) shows. We calculate the topological index (Chern number) following a method for multiband systems²⁸ and obtain $C = +1$, indicating that one MF exists. The energy spectrum for an infinite ribbon in the yy (or xx) direction is shown in figure 2, where the MF is clearly seen at longitudinal momentum π . If we consider the Andreev problem for a N/S interface along yy , we expect the MF to be detected when the incident electrons have transverse momentum $k_y = \pi$ and thus traverse only one FS pocket, at $(0, \pi)$.

By reversing the sign of the hopping parameter t_2 , a topologically trivial phase is obtained, with zero Chern number, and the FS now contains 4 pockets, as can be seen from the right panel of figure 1, and no MF's should exist.

One can also consider even parity pairing, which is realized by changing the τ matrix in (13) to $\hat{\Delta}(\mathbf{k}) = d_z(\mathbf{k})\sigma_1 \otimes \tau_3$. A direct computation of the ribbon spectrum and Chern number yields the same topological indices as before. The ribbon spectrum remains gapped in the vicinity of $k = \pi$, displaying the same edge mode, similar to that in Figure 2. This case lies outside the conditions of the theorem proved above.

From equations (4) and (13) it is clear that the Hamiltonian for each subspace has the chiral properties²⁹:

$$r_1 H(\mathbf{k}) r_1 = -H(\mathbf{k}) \quad \text{if} \quad k_x = 0, \pi, \quad (14)$$

$$r_2 H(\mathbf{k}) r_2 = -H(\mathbf{k}) \quad \text{if} \quad k_y = 0, \pi. \quad (15)$$

In either case one can rotate H to the off-diagonal form,

$$U^{\dagger} H(\mathbf{k}) U = \begin{pmatrix} 0 & A \\ A^{\dagger} & 0 \end{pmatrix}. \quad (16)$$

The matrix U is composed of the column eigenvectors of r_1 or r_2 , for each of the chiralities (14)-(15), yielding

$$A_1(k_y) = -\Xi_{\sigma} + \hat{\Delta}, \quad (17)$$

$$A_2(k_x) = -\Xi_{\sigma} + i\hat{\Delta}, \quad (18)$$

respectively. The phase of the determinant of $A_{1(2)}$ accumulates an amount $2\pi W_{1(2)}$, as its argument, $k_{y(x)}$, goes from $-\pi$ to π . The integer W is the winding number.

For the choices $\tau_j = \tau_{0,3}$ in equation (3) and $t_2 = -0.08$ (topological case), we obtain $W_2(k_y = \pi) = 1$ and $W_1(k_x = \pi) = -1$. If $t_2 = +0.08$ (non-topological case), then all $W_{1,2} = 0$. For zero k_x or k_y , we obtain $W_{1(2)} = 0$. This agrees with the existence of a single MF mode with momentum π along a ribbon, identified above.

From Figure 1 it is apparent that the FS pockets are approximately related through the nesting vector $\mathbf{Q} = (0, \pi)$ or $(\pi, 0)$, so one can ask about the effect of a charge (or spin) density wave (CDW or SDW) on the topological properties. In the case of a SDW, we keep s_z as a good quantum number. The Chern numbers remain the same as before, the spectrum remains gapped and similar to that in Figure 2. From the point of view of the winding numbers, however, there are quantitative changes in the case of a CDW. If, for instance, $\mathbf{Q} = (0, \pi)$ then the original BZ folds such that $\pi/2 < k_y < \pi/2$. For the topological case, $t_2 = -0.08$, we obtain $W_1(k_x = \pi) = -2$ and $W_1(k_x = 0) = 0$. This means that the MF still has momentum π along a ribbon in the xx direction. The winding number $W_2(k_y = 0) = 1$ because the points $k_y = 0, \pi$ are the same under the BZ folding. The MF has zero momentum for a ribbon along \mathbf{Q} , because of the BZ folding.

In the case of a SDW, the Hamiltonian in equation (4) acquires a term proportional to r_0 and no longer enjoys the chiral properties discussed.

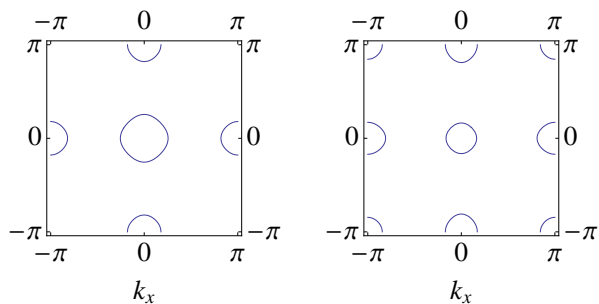


FIG. 1: Normal phase FS pockets for model (12)-(13), with $t_2 = -0.08$ (left, topological) and $t_2 = 0.08$ (right, non-topological).

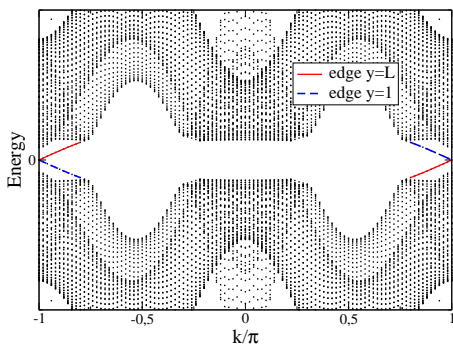


FIG. 2: Spectrum for a ribbon geometry. $\Delta = 0.1$, $t_2 = -0.08$. The edge modes containing the MF are displayed in color.

C. Induced pairing

If pairing in the multiorbital superconductor is induced by a proximity effect, it would be desirable to know the possible matrices τ_j in equations (3) and (4). Such a way of engineering a $p + ip$ superconductor has been discussed for single-band systems⁸ and, more recently, for s-wave superconductors coupled to Weyl semi-metals³⁰. A recent study³¹ of the induced pairing symmetries in a topological insulator's surface has been made, in which pseudospin degree of freedom is taken into account. It was found that a conventional local s-wave superconductor can still induce spin triplet $p + ip$ pairing, due to spin-momentum locking. In our model above there is no spin-momentum locking and induced $p + ip$ from a conventional s-wave superconductor is not expected. However, if a Rashba-type spin-orbit term is included in Hamiltonian (2), then spin-momentum locking will exist and the Chern number in equation (11) will not be affected as long as the energy gap is not closed.

Suppose the Hamiltonian $\mathcal{H}(\Delta = 0)$ of the multiorbital normal 2D system, in equations (2) and (12), is coupled to a single band superconductor \hat{H}_s through a tunneling

term \hat{T} ,

$$\hat{H}_s = \sum_{\mathbf{k}, \sigma} (\epsilon(\mathbf{k}) - \mu) \hat{b}_{\mathbf{k}, \sigma}^\dagger \hat{b}_{\mathbf{k}, \sigma} + \Delta_{\sigma\sigma'}(\mathbf{k}) \hat{b}_{\mathbf{k}, \sigma}^\dagger \hat{b}_{-\mathbf{k}, \sigma'}^\dagger + \text{H.c.}, \quad (19)$$

$$\hat{T} = \sum_{\mathbf{k}, j=1,2} V_j \hat{c}_{j, \mathbf{k}\sigma}^\dagger b_{\mathbf{k}, \sigma} + \text{H.c.} \quad (20)$$

If the pairing term in equation (19) is a local spin singlet, the induced pairing in the multiorbital layer contains the even parity local spin singlet terms (in $\sigma_2\tau_{0,1}$) as well as the $p + ip$ spin *singlet*, $d_z(\mathbf{k})\sigma_2\tau_2$. The above spin triplet $p + ip$ term (13) is also induced. The latter is weaker, however, and the resulting system is not topological.

But if the pairing term in equation (19) is a $p + ip$ spin triplet, the induced triplet term (13) is stronger than the local spin singlet term ($\sigma_2\tau_0$), and the multiorbital system has the topological properties discussed above. An additional *local* spin triplet term (in $\sigma_1\tau_2$) is also induced. Other smaller $p + ip$ spin triplet terms with odd (even) parity, in $d_z(\mathbf{k})\sigma_1\tau_{1(3)}$, are also induced. If one of the tunneling amplitudes is larger than the other ($V_1 \gg V_2$) the induced spin singlet term is strongly suppressed.

III. THE ANDREEV PROBLEM

The Chern number predicts the existence of Majorana edge states in the superconductor. Because a Majorana operator must be its own antiparticle, it must have momentum either 0 or π along the edge. In an Andreev scattering problem, the Majorana state should appear as an Andreev bound state with transverse momentum (*i.e.* along the interface) 0 or π .

In the framework of single band BTK theory, each Fermi pocket should contain one zero energy Andreev bound state. This is because the pairing function is odd, so that the electrons feel a sign change in the gap function upon specular reflection at the superconductor's surface³². Thus 3 or 4 ABS's or MF's are predicted by BTK theory, at conflict with the topological properties. The single MF observed when only a single FS pocket is crossed implies that somehow the two Andreev bound states predicted by BTK theory for the pockets (0,0) and (π ,0) should interfere destructively when the incident electron has transverse momentum $k_y = 0$.

We consider a N/S boundary along yy axis. In the framework of QWT^{17,18}, the incident electron from a single band normal metal will split into the two pseudo-spin channels of the superconductor, as figure 3 explains. In the *N* side, $x \leq 0$, the wavefunction for electrons near the Fermi level is $\exp[ik_y y]\psi_N$ where

$$\psi_N(x \leq 0) = \begin{pmatrix} 1 \\ 0 \end{pmatrix} e^{ip_+x} + b \begin{pmatrix} 1 \\ 0 \end{pmatrix} e^{-ip_+x} + a \begin{pmatrix} 0 \\ 1 \end{pmatrix} e^{ip_-x}. \quad (21)$$

The momenta p_\pm are close to the Fermi momentum p_F and are fixed by the energy, E . The amplitudes for elec-

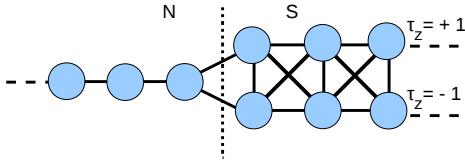


FIG. 3: Tight-binding showing the splitting of the incoming electron into two pseudo-spin channels of the superconductor, similar to a waveguide.

tron reflection, b , and Andreev hole reflection, a , allow us to obtain the differential conductance as $g_s = 1 + |a|^2 - |b|^2$, whereas the normal state conductance is just $g_n = 1 - |b|^2$. We shall consider here only $k_y = 0$ or π . The transmitted waves into the superconductor are superpositions of wavevectors \mathbf{k}^\pm , \mathbf{q}^\pm from two FS pockets (see figure 1) and the wavefunction for $x \geq 0$ is $\exp[ik_y y]\psi_S$ where

$$\begin{aligned} \psi_S(x \geq 0) = & C\phi_{\mathbf{k}^+}e^{ik^+x} + D\phi_{\mathbf{k}^-}e^{-ik^-x} \\ & + E\phi_{\mathbf{q}^+}e^{iq^+x} + F\phi_{\mathbf{q}^-}e^{-iq^-x}, \end{aligned} \quad (22)$$

where each $\phi_{\mathbf{k}}$ denotes a four-dimensional column eigenvector of the BdG matrix, H . The x-components of the momenta, k^\pm , q^\pm , are chosen so that the group velocity is positive for energy E above the gap. For subgap energies, the momenta have a positive imaginary part.

In QWT the matching conditions for wave functions (21) and (22) at $x = 0$ are written as^{17,18}

$$\psi_N(0) \otimes \begin{pmatrix} 1 \\ 1 \end{pmatrix} = \psi_S(0), \quad (23)$$

$$\partial_{k_x} \hat{H}_N \psi_N(0) = \begin{pmatrix} 1 & 1 & 0 & 0 \\ 0 & 0 & 1 & 1 \end{pmatrix} \cdot \partial_{k_x} \hat{H}_S \psi_S(x=0). \quad (24)$$

Here, H_N denotes a BdG Hamiltonian matrix for the normal metal. Interface disorder can be accounted for¹⁷ by making the replacement: $1 - b \rightarrow 1 - b - 2iZ(1 + b)p_F/p_+$ and $a \rightarrow a(1 - 2iZp_F/p_+)$ in the right-hand side of equation (24), and where Z denotes the BTK parameter²³.

IV. RESULTS

According to QWT¹⁷, the condition for the existence of ABS is obtained from the 4x4 matrix Λ composed of the four column vectors $\phi_{\mathbf{k}^+}$, $\phi_{\mathbf{k}^-}$, $\phi_{\mathbf{q}^+}$, $\phi_{\mathbf{q}^-}$, in equation (22). The condition then reads

$$\text{Det } \Lambda = 0. \quad (25)$$

We checked that condition (25) does not hold for transverse momentum $k_y = 0$ either in the topological ($t_2 =$

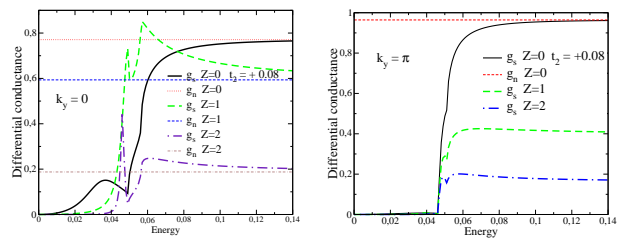


FIG. 4: Differential conductance at normal incidence (left) and for $k_y = \pi$ (right). Model (12) -(13) with $\Delta = 0.1$ and $t_2 = 0.08$ (non-topological). Dashed line: normal state differential conductance.

-0.08) or in the non-topological case ($t_2 = +0.08$). For transverse momenta $k_y = \pi$, equation (25) is verified only in the topological case. This means that the quantum interference effects from the two FS pockets effectively annihilate the two ABS's that would be predicted by single pocket BTK theory.

One might be tempted to read condition (25) as the requirement that the linear system in equation (23) be homogeneous and the wave function ψ_S be made to vanish³³ at the N/S boundary. This would be incorrect, however, as it would imply the conductance g_s to vanish. On the contrary, the conductance g_s is finite and independent of the disorder parameter Z at the energy value where equation (25) is obeyed^{17,23,32}.

For the non-topological case, the differential conductance at normal incidence, $k_y = 0$, is shown in figure 4 (left) as a function of energy (which in an actual experiment is obtained from the voltage bias). It is seen that the quantum interference suppresses quasi-particle transmission, g_s , as $E \rightarrow 0$ and the effect is even more pronounced as disorder increases. A similar result is obtained at $k_y = \pi$. Features such as peaks and dips are visible when the energy E crosses the superconducting gaps on the Fermi pockets.

For the topological case, the differential conductance at normal incidence, $k_y = 0$, is shown in figure 5. A similar destructive interference is observed at low energy.

For transverse momentum $k_y = \pi$, the ABS (MF) leaves its imprint on the conductance, as figure 6 shows. The differential conductance attains the maximum value $g_s = 2$ at $E = 0$, independent of Z .

V. SUMMARY AND CONCLUSIONS

We have studied a model of a multiorbital 2D superconductor which is realized by introducing $p + ip$ Cooper pairing, diagonal in the pseudospin channel, in an otherwise TI. Under these conditions, the topological properties of the TI were shown to become irrelevant. The topological properties of the multiorbital superconductor depend on the FS in the normal phase. If the FS contains several sheets, we have shown that when the number of Fermi pockets is odd, the MF is in the single pocket that

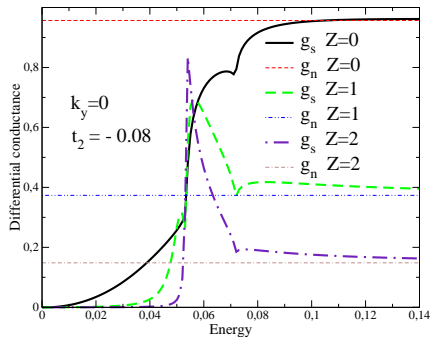


FIG. 5: Differential conductance at normal incidence, for the same model as in Figure 4 with $t_2 = -0.08$ (topological). Dashed line: normal state differential conductance.

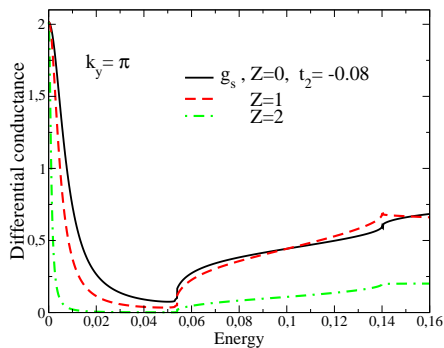


FIG. 6: Differential conductance for the topological case, showing the signature of the MF.

is traversed by the quasi-particles, while the other pair of pockets interfere destructively. This result from QWT reconciles the number of MFs with the Chern number, in contrast to BTK theory. In addition to the destruction of the MFs, the waveguide interference effects also produce a vanishing conductance at $E = 0$, when a pair of FS pockets is traversed by the quasi-particles.

VI. ACKNOWLEDGMENTS

We acknowledge the hospitality of CSRC, Beijing, China, where part of this work has been carried out. We would like to thank financial support from Fundação para a Ciência e Tecnologia (Project EXPL/FIS-NAN/1728/2013 and Grant No. PEST-OE/FIS/UI0091/2011).

-
- ¹ Hasan M. Z. and Kane C. L., *Rev. Mod. Phys.*, **82** (2010) 3045.
 - ² Araújo M. A. N., Castro E. V. and Sacramento P. D., *Phys. Rev. B*, **87** (2013) 085109.
 - ³ Qi X.-L. and Zhang S.-C., *Rev. Mod. Phys.*, **83** (2011) 1057.
 - ⁴ Alicea J., *Rep. Prog. Phys.*, **75** (2012) 076501.
 - ⁵ Ivanov D. A., *Phys. Rev. Lett.*, **86** (2001) 268.
 - ⁶ Nayak C., Simon S., Stern A., Freedman., Das Sarma S., *Rev. Mod. Phys.*, **80** (2008) 1083.
 - ⁷ Fu L. and Kane C. L., *Phys. Rev. Lett.*, **100** (2008) 096407.
 - ⁸ Potter A. and Lee P. A., *Phys. Rev. B*, **83** (2011) 184520.
 - ⁹ Wang E. *et al.*, *Nature Phys.*, **9** (2013) 621.
 - ¹⁰ Linder J., Tanaka Y., Yokoyama T., Sudbø A. and Nagaosa N., *Phys. Rev. Lett.*, **104** (2010) 067001.
 - ¹¹ Fu L. and Berg E., *Phys. Rev. Lett.*, **105** (2010) 097001.
 - ¹² Fu L., *Phys. Rev. B*, **90** (2014) 100509.
 - ¹³ Deng S., Ortiz G. and Viola L., *Phys. Rev. B*, **87** (2013) 205414.
 - ¹⁴ Deng S., Ortiz G., Poudel A. and Viola L., *Phys. Rev. B*, **89** (2013) 140507.
 - ¹⁵ Araújo M. A. N. and P. D. Sacramento P. D., *Physical Review B*, **77** (2008) 134519; **78** (2008) 229902 .
 - ¹⁶ Araújo M. A. N. and A. H. Castro Neto A. H., *Physical Review B* **75** , 115133 (2007)
 - ¹⁷ Araújo M. A. N. and Sacramento P. D., *Phys. Rev. B*, **79** (2009) 174529.
 - ¹⁸ Araújo M. A. N. and Sacramento P. D., *J. of Physics: Conf. Series* **200** 012008 (2010).
 - ¹⁹ Burmistrova A. V., Karminskaya T. Y., Devyatov I. A., *JETP Letters* **93** 133 (2011).
 - ²⁰ Burmistrova A. V. and Devyatov I. A., *JETP Letters* **95** 239 (2012).
 - ²¹ Burmistrova A. V., Devyatov I. A., Golubov A. A., Yada K., Tanaka Y., *Superconductor Science and Technology*, **27** (2014) 015010.
 - ²² Burmistrova A. V., Devyatov I. A., Golubov A. A., Yada K., Tanaka Y., *J. Phys. Soc. Japan* **82**, 034716 (2013).
 - ²³ Blonder G. E., Tinkham M. and Klapwijk T. M., *Phys. Rev. B*, **25** (1982) 4515.
 - ²⁴ Kallin C., *Rep. Prog. Phys.*, **75** (2012) 042501.
 - ²⁵ Yada K., Golubov A., Tanaka Y., Kashiwaya S., *J. Phys. Soc. Japan*, **83** (2014) 074706.
 - ²⁶ Sato M., *Phys. Rev. B*, **81** (2010) 220504.
 - ²⁷ Sato M., *Phys. Rev. B*, **79** (2009) 214526.
 - ²⁸ Hatsugai Y., Fukui T. and Aoki H., *Phys. Rev. B*, **74** (2006) 205414.
 - ²⁹ Schnyder A. P., Ryu S., Furusaki A., and Ludwig A. W. W., *Phys. Rev. B*, **78** (2008) 195125.
 - ³⁰ Khanna U., Kundu A., Pradhan S. and Rao S., *Phys. Rev.*

B, **90**, (2014) 195430.

³¹ Black-Schaffer A. M. and Balatsky A., *Phys. Rev. B*, **87** (2013) 220506(R).

³² Kashiwaya S., Tanaka Y., Koyanagi M. and Kajimura K.,

Phys. Rev B, **53** (1996) 2667.

³³ Yamakage A., Yada K., Sato M., Tanaka Y., *Phys. Rev B*, **85** (2012) 180509(R).